Representation of Border, Velocity and Speed in the Goldfish Brain

Ehud Vinepinsky[1,2], Shay Perchik[2,3], Ohad Ben-Shahar[2,4], Opher Donchin[2,5] and Ronen Segev[1,2,5,*]

[1]Life Sciences Department, Ben Gurion University of the Negev, Beer Sheva 84105, Israel

[2]Zlotowski Center for Neuroscience, Ben Gurion University of the Negev, Beer Sheva 84105, Israel

[3]Department of Cognitive and Brain Sciences, Ben-Gurion University of the Negev, Beer Sheva 84105, Israel

[4]Computer Sciences Department, Ben Gurion University of the Negev, Beer Sheva 84105, Israel

[5]Biomedical Engineering Department, Ben Gurion University of the Negev, Beer Sheva 84105, Israel

[*]correspondence: ronensgv@bgu.ac.il

Abstract

Like most animals, the survival of fish depends crucially on navigation in space. This capacity has been documented in numerous behavioral studies that have revealed navigation strategies and the sensory modalities used for navigation. However, virtually nothing is known about how fish represent space and locomotion in the brain to enable successful navigation. Using a novel wireless recording system, we measured the activity of single neurons in the goldfish lateral pallium, a brain region known to be involved in spatial memory and navigation, while the fish swam freely in a water tank. Three cell types were identified: border cells, velocity cells and speed cells. Border cells are active when the fish is near the boundary of the environment. Velocity cells encode swimming direction and speed and can represent the direction needed for navigation. Speed cells only encode the absolute speed independent of direction and may provide an odometry signal. This study is thus the first to address the question of how information relevant for navigation may be represented in the fish brain, and address the fundamental question of the neural basis of navigation in this diverse group of vertebrates. The similarities between our observations in fish and earlier findings in mammals may indicate that the networks controlling navigation in vertebrate originate from a common ancient circuit.

Navigation is a fundamental behavioral capacity facilitating survival in many animal species *(4-7)*. It involves the continuous estimation and representation of the agent's position and direction in the environment which are implemented in the planning and execution of movements and trajectories towards target locations *(8, 9)*. Navigation has been investigated extensively on numerous taxa across the animal kingdom but attempts to probe its neural substrate have mainly been focused on mammals *(10)* and insects *(11)*. In mammals, neurons in the hippocampal formation encode information about the position and orientation of the animal in space *(8-10, 12, 13)*. These cells include place cells *(14)*, grid cells *(15)*, head-direction cells *(16, 17)* and other cell types *(18, 19)*. In insects, a ring-shaped neural network in the central complex of fruit fly was shown to represent its heading direction *(11)*.

To better understand space representation in other taxa, we explored the neural substrate of navigation in the goldfish (*Carassius auratus*). These fish are known to be able to navigate either by exploiting an allocentric or an egocentric frame of reference. This may imply that the goldfish has the ability to build an internal representation of space in the form of a cognitive map *(3)*. This would include cognitive map-like navigation strategies to find a goal when starting from an unfamiliar initial position, or taking shorter alternative routes (shortcuts) when possible *(2, 3, 20, 21)*. Furthermore, goldfish use many environmental cues, such that any single cue would not be crucial in itself to navigating in the environment *(21)*.

In addition to these behavioral studies, lesion studies on goldfish have shown that the telencephalon is crucial for spatial navigation. Damage to the lateral pallium in the telencephalon leads to dramatic impairment in allocentric spatial memory and learning, but not when the lesion affects other parts of the telencephalon *(21)*. These finding are similar to results from lesions studies of the hippocampus in mammals and further confirm that the lateral pallium in goldfish is a possible homologue of the mammalian

hippocampus *(3, 22)* (but see also *(23)*). While these works have contributed to suggesting where the possible navigation mechanism is located in the brain, they have not addressed the nature of the representation of this information, the goal of this study.

To better understand how facets of space and locomotion are represented in the teleost brain, we measured single cell activity in the lateral pallium of freely behaving goldfish while they explored a water tank. We first trained the fish (13-15 cm body length) to swim back and forth in a linear tank measuring 1.4 m X 0.2 m X 0.2 m. This quasi 1D geometry was used to allow efficient data collection similar to procedures employed in rodents *(24)*. After the fish became familiar with the water tank and learned to explore its entire length naturally, we installed a recording system on their head *(1)*. We then let the goldfish swim freely while a camera positioned over the entire tank recorded the locations of the fish and a data logger recorded the activity of single cells using tetrodes (Figure 1A, see Methods).

Using this methodology, we identified three types of cells that may constitute the primitives of the goldfish navigation system, which we term border cells, velocity cells, and speed cells. Border cells are active when the fish is in close proximity to the borders of its environment (i.e., in our case near the walls of the water tank). Velocity cells are active when the fish swims in a particular direction and speed, regardless of position. Speed cells become active when the fish swims faster regardless of position or direction.

Several examples of border cells from the lateral pallium of different goldfish are presented in Figure 1 B-J. The fish's trajectory (black curve, Figure 1B) is presented together with the location of the fish when each spike of a single cell occurred (red dots). The emerging pattern shows that this neuron was mainly active when the fish

was near the boundaries of the tank. This was also documented by the color-coded heat map of the firing pattern of the neuron (Figure 1C; the recording location in the brain is presented in Figure 1D and the spike shapes are presented in Figure 1E). To test whether a neuron was a border cell we first defined the width of the border activity layer as the distance from the walls in which 75% of the spikes occurred. Then, we employed a standard shuffling procedure where we obtained shuffled spike trains and measured the border activity layer of each of the shuffled trains. Then by comparing the border activity layer of the cell to the shuffled data we obtained the confidence interval of the result ($p<0.005$, Figure 1F, see Methods). Additional examples of border cells can be found in Figure 1G-J and Supplementary Figure 1. Analysis showed that 48 out of 132; i.e., 36% of all the well-isolated units recorded in 15 fish could be classified as border cells.

Velocity cells fire in correlation to the direction and speed of the fish while swimming. Thus, this cell type represents locomotion in space in an allocentric; i.e., world centered, coordinate system. Examples of velocity cells are presented in Figure 2. Although the fish's trajectory and neuronal activity do not seem to represent any particular pattern (Figure 2A), a pattern nevertheless emerges when the analysis is dissected by the longitudinal component (horizontal in the figure) of motion in the water. Some velocity cells were more active when the fish swam rightwards, and others did so for leftward motion. Figure 2B shows a cell with preferred motion to the right. This was also apparent when we examined the tuning of neuronal activity as function of the velocity along the longitudinal axis vs. time (Figure 2C) where this neuron encoded the velocity; i.e., the direction and magnitude of motion on the horizontal axis (see Supplementary Figure 2A for the color-coded firing rate map as a function of the two dimensional velocity). To test statistically whether a neuron was a velocity cell, we employed a standard shuffling procedure (Figure 2D, $P<0.005$, see Methods).

A cell from a different fish with tuning to the left is presented in Figure 2E-H (with two-dimensional velocity tuning; see Supplementary Figure 2B). Additional examples are presented in Supplementary Figure 3. We found that 20 out of 132; i.e., 15% of all units recorded in 15 fish could be classified as velocity cells.

Speed cells are tuned to the absolute value of the velocity. This cell type represents locomotion in an egocentric coordinate system and may be used as an odometry signal. Two examples of speed cells are presented in Figure 3. Again, the activation of cells during the trajectory did not reveal any apparent pattern (Figure 3 A and F). However, when the firing rate map was considered in the velocity space, a pattern showing tuning to speed emerged, revealing that the firing rate increased with the speed regardless of the direction of motion (Figure 3 B and C, Figure 3 G and H).

The correlation coefficient between the neuronal firing rate and fish speed was calculated and a standard shuffling procedure was used to test for speed selectivity of the neurons (see Methods). The correlation coefficient between firing rate and velocity showed no statistically significant pattern (Figure 3 D and E, I and J). Analysis indicated that 33 out of 132; i.e., 25% of all well-isolated units recorded in 15 fish could be classified as speed cells.

The border, velocity and speed cells form overlapping populations. This was confirmed by using a standard shuffling procedure to test for conjunction of tuning. The tuning curves for two selected cells are presented in Figure 4. One cell encoded both border and velocity (Figure 4A-E); another cell encoded both border and speed (Figure 4F-L).

The total number of different functional cell types recorded in the goldfish is presented in Figure 5A. This includes border, velocity, speed and conjunction border-velocity and border-speed classes.

In addition, for five of the fish we located the recording location using standard post-recording anatomical procedures (see Methods). Border cells were found only below the Dlv/Dp boundary (Figure 5B), which is consistent with neuroanatomy *(25-27)* that distinguishes these regions from the regions above them (Dld and Dd). Note that the division between the Dlv and Dp is a topic of ongoing debate *(25-27)* and previous conclusions regarding the anatomical localization of cell types can also be influenced by lesion resolution.

In summary, we found border, velocity and speed cells that represent different components of position and locomotion in the goldfish brain. These neurons were found in the Dlv/Dp and Dd, indicating that these regions contain a variety of neurons that represent features of space, direction and speed. These cell types may be the basic building blocks of the goldfish navigation system and can thus shed new light on theories of navigation systems based on observations of the mammalian system alone. This study is the first step in identifying the functional properties of cells in the lateral pallium. Further investigations are needed to obtain a complete functional map of this region and understand its foundational role in the neural navigation system of the teleost brain.

These results have important implications for current theories on of the evolution of brain function in the teleost and outside the teleost lineage. Lesion studies in the goldfish brain suggest that the lateral pallium and specifically the Dlv is the homolog of the mammalian hippocampus. The border, velocity and speed cells we found have counterparts in the mammalian Medial Entorhinal Cortex and Subiculum *(10)*. This suggests that the actual homolog of the Dlv is the hippocampal formation that contains several sub-regions in the mammalian brain which includes the hippocampus, the Entorhinal Cortex, the Subiculum and the post-Subiculum *(28)*. Currently however, it

is impossible to determine the exact homology between the divisions of the mammalian hippocampal formation and the divisions of the pallium in the teleost brain. In addition, it is not clear whether there is such a division. Given the imbalance of what is known about on the connectivity maps in the two lineages, fish brain connectivity is poorly understood as compared to the relatively well-known connectivity of the mammalian brain *(28)*.

Although there is a robust consensus regarding the inventory of cells that represent space in the mammalian brain *(8, 10, 13)*, there is no accepted theory, based on empirical data, explaining how these components of spatial representations are integrated in the brain into a functioning navigation system *(8)*. One solution can emerge from studying the neural mechanisms underlying navigation in other vertebrate lineages, since elucidating the mechanisms of space representation in different vertebrate taxa can help decipher how the elementary building blocks of navigation are integrated into a functional navigation system *(29-33)*. Crucially, comparative studies can help determine whether the mammalian navigation system is unique or an instance of a more general biological design. Thus, a comparative approach may help resolve the key question of the critical components making up a functioning navigation system.

The small number of past attempts in this direction are inconclusive. In particular, technical problems have impeded studies on space representation in the pigeon brain *(34)* and in fish *(35, 36)*. Works investigating space representation the fruit fly suggest it can represent orientation with respect to a salient landmark in the environment *(11, 37)*.

To conclude, our study is the first step toward understanding the navigation system in non-mammalian vertebrates. This could lead to a better understanding of the basic building block of this system across all vertebrates.

Methods

Animals. All goldfish experiments were approved by the Ben-Gurion University of the Negev Institutional Animal Care and Use Committee and were in accordance with government regulations of the State of Israel. Goldfish (Carassius auratus), 13–15 cm in body length, 80-120 g body weight were used in this study. A total of 15 fish were used for the recordings. The fish were kept in a water tank at room temperature. The room was illuminated with artificial light on a 12/12 h day-night cycle. Fish were kept in the home water tank and were brought to the experimental water tank for recordings.

Wireless electrophysiology. The behavioral fish electrophysiology is described in detail in Vinepinsky et al. *(1)*. Briefly, the experimental setup for recording extracellular signals from the brain of freely swimming goldfish is based on a small data logger (Mouselog-16, Deuteron Technologies Ltd., Jerusalem, Israel) connected to an implant on the fish's skull and receive input from one or two tetrodes that are mounted in the fish brain. To protect the electronics, the neural logger is placed in a waterproof case (Figure 1A). The data logger is controlled wirelessly by a computer via a transceiver (Deuteron Technologies Ltd., Jerusalem, Israel) and records the neural signals for up to 4 hours per session. The fish's behavior is monitored continuously with a video camera positioned over the tank. The video is synchronized with the recording by feeding a trigger signal from the logger into the camera. A styrofoam marker mounted on the box which contains the logger to make the entire implant (tetrodes, box, logger and battery) buoyancy neutral (i.e. total average density of 1 gr/cm^3). The front and back ends of the styrofoam marker were painted in different colors to easily determine the swimming direction automatically from the video recordings. A total of 132 neurons in 15 fish were monitored.

Spike sorting was done using manual clustering based on the spikes amplitude, width, and waveforms across all the electrodes in the tetrode. All analyses were implemented using an in-house Matlab program.

Water tank. The water tank for the experiment was 1.4 m X 0.2 m X 0.2 m in size and coated with white plastic sheets. A camera above the water tank was used to localize the fish in the X-Y plane. Each of the two long walls of the water tank were marked with 4 shapes that served as visual landmarks.

Training. Prior to surgery, the fish were trained to explore the tank back and forth. Training was obtained in some cases by allowing the fish to swim freely in the tank for one hour a day for several days, and in other cases by using automatic feeders positioned at both ends of the task that fed the fish as soon as it approached the corresponding end. In both cases the goldfish usually learned to swim back and forth after about a week of training. After training, the fish underwent the surgery to implant the tetrodes and the logger case.

Recording sessions. Each recording session included synchronized recording from the Neurolog-16 and the camera system while the fish navigated freely in the water tank. Recording sessions lasted 30 min to 2 hours.

Analysis. After the experiment, the data from the cameras and the Neurolog-16 were analyzed. This was done by detecting the action potential timing using a standard spike-sorting algorithm *(38, 39)*. Then the correlation coefficients between the fish's behavior, location and orientation, and the neural activity were calculated to determine how space was represented during the task. Subsequently, the brain of five of the fish were fixed and sliced to reveal the electrode position in the brain (i.e. the lateral pallium or any other brain area targeted for recording).

Data analysis: Fish trajectory and firing rate map. The fish's location in each video frame was detected using the colored styrofoam marker that was attached to the case containing the logger. The water tank was tessellated to 1 cm^2 bins and smoothed using a 2- dimensional Gaussian (σ = 5 cm). This yielded two auxiliary maps, which indicated how many spikes occurred in each bin and how much time the fish spent in each bin. The firing rate map for each neuron was obtained by dividing the two maps bin by bin. Bins that were not visited at all by the fish were discarded from the analysis and appear on the map as white bins.

Data analysis of border cells: To determine which cells could be classified as border cells, we measured the width of the border activity layer near the walls of the water tank which contained 75% of the spikes. We compared this to 5000 shuffled spike trains. Each shuffled spike train was obtained by first calculating the inter-spike intervals, shuffling the inter-spike intervals by random permutation and using the cumulative sum to obtain the shuffled spike train. Then we calculated the probability of observing a width of border activity layer by comparing the value obtained for the recorded cell to the values calculated for the shuffled spike trains. Cells with a p value below 0.005 and an activity layer less than 5 cm were considered to be border cells. Sensitivity analysis on the fraction of spikes the activity layer should contain was done by calculating the activity layer, which contained 0-100% of the spikes (Supplementary Figure 1). We also compared the border measure to ones used by in other studies *(18)* (Supplementary Figure 5), and found that our measure was more sensitive for cells with low firing rates such as the ones in the goldfish pallium.

Data analysis of velocity cells. To classify velocity cells, we measured the correlation coefficient between the cellular firing rate and the velocity of the fish. Then 5000 shuffled spike trains were obtained by first calculating the inter-spike intervals, shuffling

the inter-spike intervals by random permutation and using the cumulative sum to obtain a shuffled spike train. For each shuffled spike train, the correlation coefficient between the firing rate and fish velocity was calculated. By comparing the result of the shuffled spike trains to the cellular result, we obtained an estimate of the p-value of each cell. By definition, velocity cells could meet the statistical criterion for speed cells. Therefore, cells that met the velocity criterion were removed from the speed cell group.

Data analysis of speed cells. To classify speed cells, we measured the correlation coefficient between the cellular firing rate and the speed of the fish. Then 5000 shuffled spike trains were obtained by first calculating the inter-spike intervals, shuffling the inter-spike intervals by random permutation and using the cumulative sum to obtain the shuffled spike train. For each shuffled spike train the correlation coefficient between the firing rate and fish speed was calculated. Comparing the result of the shuffled spike trains to the cellular result yielded an estimate of the p-value of each cell.

Testing for information encoded in neural activity. To test for the spatial encoding properties of cells we calculated the information per spike (measured in bits per spike) for all cells *(15, 40)*. This was done by calculating the mutual information between fish position and the neural activity, as follows:

$$I(Position, Spikes) = H(Position) - H(Position|Spikes)$$

where $H(X) = -\sum_X P(X) log_2(P(X))$ is the entropy of any random variable *X*. The space was divided into bins and only bins where the fish spent at least 1 second during the experiment were taken into account. All cells with information ≥0.5 bits/spike were used for further analysis where we tested for border encoding properties. We did not found cells that crossed the information criterion that were not classified as border cells.

Acknowledgments

We are grateful to Jacob Vecht from Deuteron Technologies Ltd and the members of the Ulanovsky lab for all their help in setting up the recording system for behaving fish. In addition, we are grateful to Mario Wullimann for guidance in interpreting the anatomical data and Tal Novoplansky-Tzur for helpful technical assistance. We gratefully acknowledge financial support from THE ISRAEL SCIENCE FOUNDATION – FIRST Program (grant no. 281/15), the Frankel center at the Computer Science Department, and the Helmsley Charitable Trust through the Agricultural, Biological and Cognitive Robotics Initiative of Ben-Gurion University of the Negev.

Figure captions

Figure 1| Border cells in the goldfish lateral pallium. A. Schematic overview of the experimental setup: a fish swims freely in a water tank with electrodes and a wireless data logger mounted on its head. The fish's movements are recorded by a video camera positioned above the tank. **B.** An example of a border cell. The fish trajectory (black curve) is presented together with the location of the fish when each spike of a single cell occurred (red dots). The apparent pattern shows that this neuron was mainly active when the fish was at the boundaries of the tank. **C.** Firing rate map of the cell in **B**., color-coded from zero (blue) to maximum firing rate (red). The highest spiking probabilities are concentrated at the boundaries. **D.** Tetrode position of the cell in **A,** recording was made from the Dlv part of the telencephalon in this experiment. **E.** Spike waveforms of the cell in **A**. **F.** Statistical analysis of firing near the border of the water tank. Border activity layer of shuffled spike trains are contrasted with the border activity layer of the cell in **A** marked by the arrow. **G-K.** Four additional examples of border cells from four different fish.

Figure 2| Velocity cells in the goldfish lateral pallium. A. Trajectory (black curve) and activity map (red dots) of a velocity neuron. **B.** Trajectory and activity map along the longitudinal axis: the neuron was more active when the fish swam rightward. **C.** Firing rate of the cell in A as a function of velocity in the longitudinal direction. The cell is tuned to the velocity in the positive direction. **D.** Correlation coefficient between the firing rate of the cell in **A**. and the fish velocity vs. 5000 shuffled spike trains. **E-H.** Another example of a velocity cell from another experiment. This cell is tuned to the velocity in the negative direction.

Figure 3| Speed cells in the goldfish lateral pallium. A. Trajectory (black curve) and activity map (red dots) of a speed neuron. **B.** Firing rate of the cell in **A**. as a function of velocity in the longitudinal direction. The cell is tuned to speed in both directions. **C.**

Speed tuning curve of the cell in **A**.; firing rate as a function of the fish's speed. The firing rate increases with the speed. **D.** The correlation coefficient between firing rate and speed for the cell in **A** (red arrow) vs. the correlation coefficient of the firing rate and the speed of 5000 shuffled spike trains. **E.** Analysis of correlation between the firing rate and fish velocity of the cell in **A**. (red arrow) vs. 5000 shuffled spike trains. The firing rate is correlated to speed and not direction. **F-J.** Another example of a speed cell from another experiment.

Figure 4| Mixed selectivity cells. Border-Velocity cell (A-E). A. Fish trajectory and activity map together with the firing rate heat map. **B.** Firing rate of the cell in **A.** as a function of velocity in the longitudinal direction. **C.** Statistical analysis of the border activity layer. **D.** Statistical analysis of the correlation coefficient between velocity and firing rate. **E.** Joint distribution of the border activity layer and the correlation coefficient between velocity and firing rate acquired by 1000^2 shuffled spike trains. Red lines represent the marginal 99.5 percentiles. The value of the cell in **A**. is marked by a red star. **Border-Speed cell (F-L). F.** Fish trajectory and firing rate heat map. **G.** Firing rate of the cell in **A**. as a function of velocity in the longitudinal direction. **H.** Speed tuning of the cell. **I.** Statistical analysis of the border activity layer. **J.** Statistical analysis of the correlation coefficient between fish speed and firing rate. **K.** Joint distribution of the border activity layer and the correlation coefficient between fish speed and firing rate acquired by 1000^2 shuffled spike trains. Red lines represent the marginal 99.5 percentiles. The value for the cell in **F** is marked by a red star. **L.** Statistical analysis of the correlation coefficient between velocity and firing rate. The firing rate is correlated to speed and not direction.

Figure 5| Distribution of cells in the goldfish brain. A. Distribution of cells in our recordings **B.** Summary of the locations we recorded from in five fish and the type of

cells we found in these locations. The border cells were only identified after crossing into the Dlv/Dp region (anatomy diagram based on Northchutt *(25)*).

References

1. A. Tsoar *et al.*, Large-scale navigational map in a mammal. *Proc. Natl. Acad. Sci. U. S. A.* **108**, E718-24 (2011).

2. R. Wehner, Desert ant navigation: how miniature brains solve complex tasks. *Journal of Comparative Physiology A: Neuroethology, Sensory, Neural, and Behavioral Physiology.* **189**, 579-588 (2003).

3. A. Dittman, T. Quinn, Homing in Pacific salmon: mechanisms and ecological basis. *J. Exp. Biol.* **199**, 83-91 (1996).

4. H. Lipp *et al.*, Pigeon homing along highways and exits. *Current Biology.* **14**, 1239-1249 (2004).

5. B. L. McNaughton, F. P. Battaglia, O. Jensen, E. I. Moser, M. Moser, Path integration and the neural basis of the'cognitive map'. *Nature Reviews Neuroscience.* **7**, 663-678 (2006).

6. E. I. Moser, E. Kropff, M. Moser, Place cells, grid cells, and the brain's spatial representation system. *Annu. Rev. Neurosci.* **31**(2008).

7. E. I. Moser *et al.*, Grid cells and cortical representation. *Nature Reviews Neuroscience.* **15**, 466-481 (2014).

8. J. D. Seelig, V. Jayaraman, Neural dynamics for landmark orientation and angular path integration. *Nature.* **521**, 186-191 (2015).

9. G. Buzsáki, E. I. Moser, Memory, navigation and theta rhythm in the hippocampal-entorhinal system. *Nat. Neurosci.* **16**, 130-138 (2013).

10. D. C. Rowland, Y. Roudi, M. Moser, E. I. Moser, Ten years of grid cells. *Annu. Rev. Neurosci.* **39**, 19-40 (2016).

11. J. O'Keefe, J. Dostrovsky, The hippocampus as a spatial map. Preliminary evidence from unit activity in the freely-moving rat. *Brain Res.* **34**, 171-175 (1971).

12. T. Hafting, M. Fyhn, S. Molden, M. Moser, E. I. Moser, Microstructure of a spatial map in the entorhinal cortex. *Nature.* **436**, 801-806 (2005).

13. J. S. Taube, R. U. Muller, J. B. Ranck Jr, Head-direction cells recorded from the postsubiculum in freely moving rats. I. Description and quantitative analysis. *J. Neurosci.* **10**, 420-435 (1990).

14. J. S. Taube, R. U. Muller, J. B. Ranck Jr, Head-direction cells recorded from the postsubiculum in freely moving rats. II. Effects of environmental manipulations. *J. Neurosci.* **10**, 436-447 (1990).

15. T. Solstad, C. N. Boccara, E. Kropff, M. B. Moser, E. I. Moser, Representation of geometric borders in the entorhinal cortex. *Science.* **322**, 1865-1868 (2008).

16. E. Kropff, J. E. Carmichael, M. Moser, E. I. Moser, Speed cells in the medial entorhinal cortex. *Nature.* **523**, 419-424 (2015).

17. F. Rodriguez *et al.*, Conservation of spatial memory function in the pallial forebrain of reptiles and ray-finned fishes. *J. Neurosci.* **22**, 2894-2903 (2002).

18. C. Broglio, F. Rodriguez, C. Salas, Spatial cognition and its neural basis in teleost fishes. *Fish Fish.* **4**, 247-255 (2003).

19. C. Broglio, A. Gómez, E. Durán, C. Salas, F. Rodríguez, Brain and cognition in teleost fish. *Fish Cognition and Behavior.*, 325-358 (2011).

20. C. Salas *et al.*, Neuropsychology of learning and memory in teleost fish. *Zebrafish.* **3**, 157-171 (2006).

21. F. Rodrıguez *et al.*, Spatial memory and hippocampal pallium through vertebrate evolution: insights from reptiles and teleost fish. *Brain Res. Bull.* **57**, 499-503 (2002).

22. S. B. Elliott, E. Harvey-Girard, A. C. Giassi, L. Maler, Hippocampal- like circuitry in the pallium of an electric fish: Possible substrates for recursive pattern separation and completion. *J. Comp. Neurol.* **525**, 8-46 (2017).

23. Y. Ziv *et al.*, Long-term dynamics of CA1 hippocampal place codes. *Nat. Neurosci.* **16**, 264 (2013).

24. E. Vinepinsky, O. Donchin, R. Segev, Wireless electrophysiology of the brain of freely swimming goldfish. *J. Neurosci. Methods.* **278**, 76-86 (2017).

25. R. G. Northcutt, Connections of the lateral and medial divisions of the goldfish telencephalic pallium. *J. Comp. Neurol.* **494**, 903-943 (2006).

26. M. F. Wullimann, E. Rink, The teleostean forebrain: a comparative and developmental view based on early proliferation, Pax6 activity and catecholaminergic organization. *Brain Res. Bull.* **57**, 363-370 (2002).

27. T. Mueller, M. F. Wullimann, An evolutionary interpretation of teleostean forebrain anatomy. *Brain Behav. Evol.* **74**, 30-42 (2009).

28. A. B. Butler, W. Hodos, *Comparative vertebrate neuroanatomy: evolution and adaptation* (Wiley. com, , 2005).

29. M. M. Yartsev, N. Ulanovsky, Representation of three-dimensional space in the hippocampus of flying bats. *Science.* **340**, 367-372 (2013).

30. A. Finkelstein, L. Las, N. Ulanovsky, 3-D maps and compasses in the brain. *Annu. Rev. Neurosci.* **39**, 171-196 (2016).

31. M. M. Yartsev, M. P. Witter, N. Ulanovsky, Grid cellswithout theta oscillations in the entorhinal cortex of bats. *Nature.* **479**, 103 (2011).

32. N. Ulanovsky, C. F. Moss, Hippocampal cellular and network activity in freely moving echolocating bats. *Nat. Neurosci.* **10**, 224-233 (2007).

33. A. Sarel, A. Finkelstein, L. Las, N. Ulanovsky, Vectorial representation of spatial goals in the hippocampus of bats. *Science.* **355**, 176-180 (2017).

34. V. P. Bingman, G. E. Hough 2nd, M. C. Kahn, J. J. Siegel, The homing pigeon hippocampus and space: in search of adaptive specialization. *Brain Behav. Evol.* **62**, 117-127 (2003).

35. M. B. Ahrens, K. H. Huang, S. Narayan, B. D. Mensh, F. Engert, Two-photon calcium imaging during fictive navigation in virtual environments. *Front. Neural Circuits.* **7**, 104 (2013).

36. J. G. Canfield, S. J. Mizumori, Methods for chronic neural recording in the telencephalon of freely behaving fish. *J. Neurosci. Methods.* **133**, 127-134 (2004).

37. A. G. Varga, R. E. Ritzmann, Cellular basis of head direction and contextual cues in the insect brain. *Current Biology.* **26**, 1816-1828 (2016).

38. R. Segev, J. Goodhouse, J. Puchalla, M. J. Berry, Recording spikes from a large fraction of the ganglion cells in a retinal patch. *Nat. Neurosci.* **7**, 1155-1162 (2004).

39. M. S. Lewicki, A review of methods for spike sorting: the detection and classification of neural action potentials. *Network: Comput. Neural Syst.* **9**, 53-78 (1998).

40. N. Ulanovsky, C. F. Moss, What the bat's voice tells the bat's brain. *Proc. Natl. Acad. Sci. U. S. A.* **105**, 8491-8498 (2008).

Figure 1 – Vinepinsky et al

Border Cells

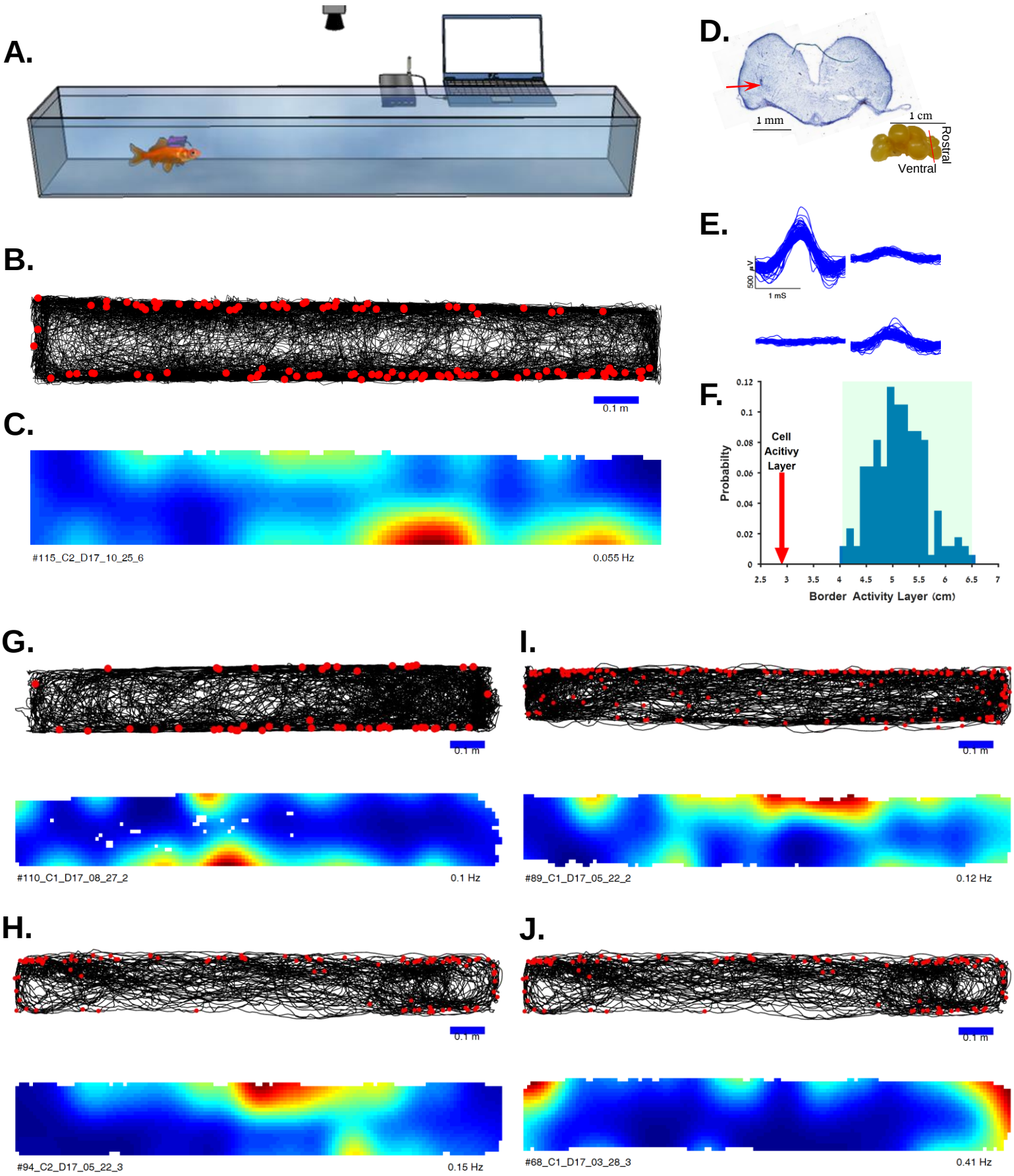

Figure 2 – Vinepinsky et al

Velocity Cells

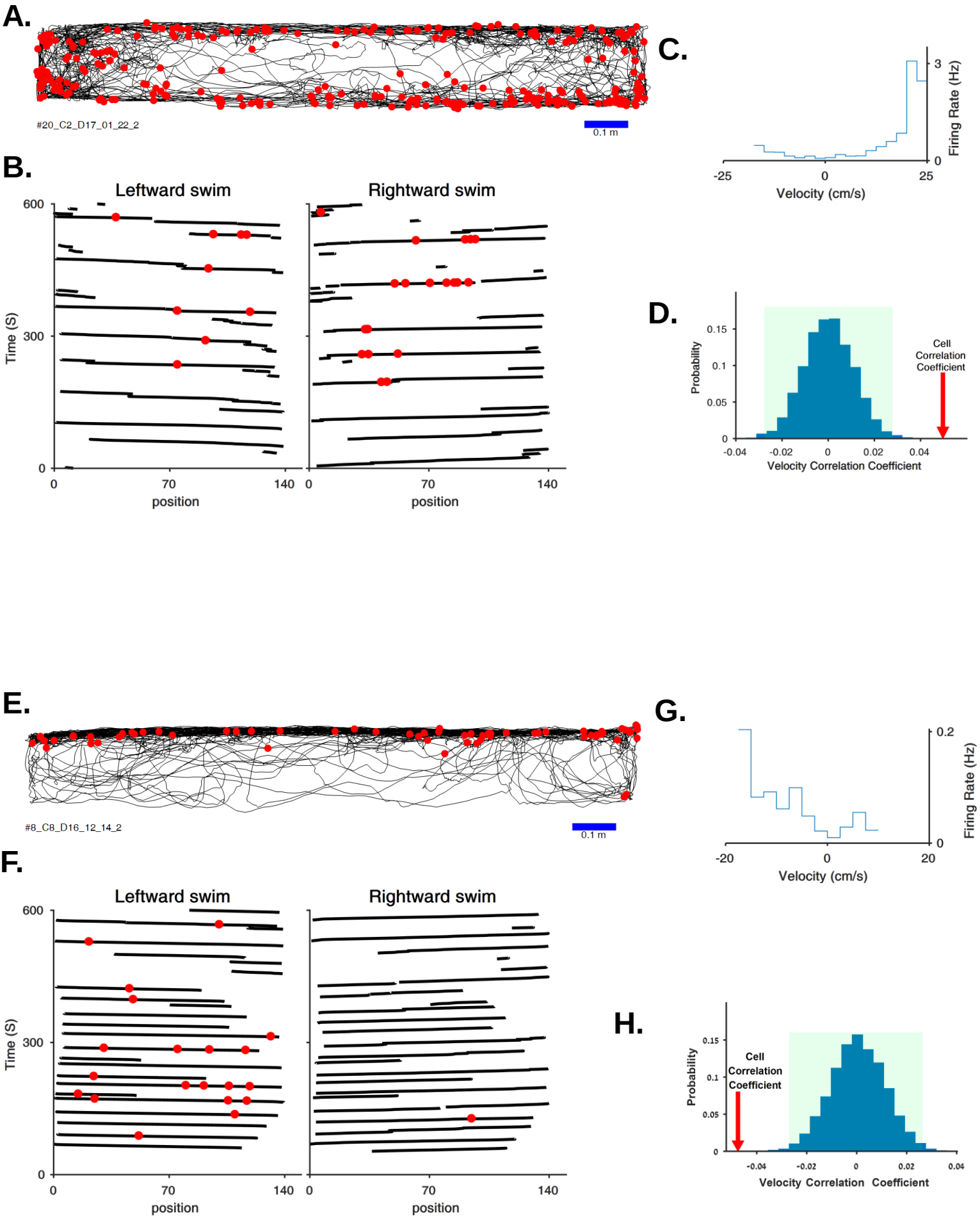

Figure 3 – Vinepinsky et al

Speed Cells

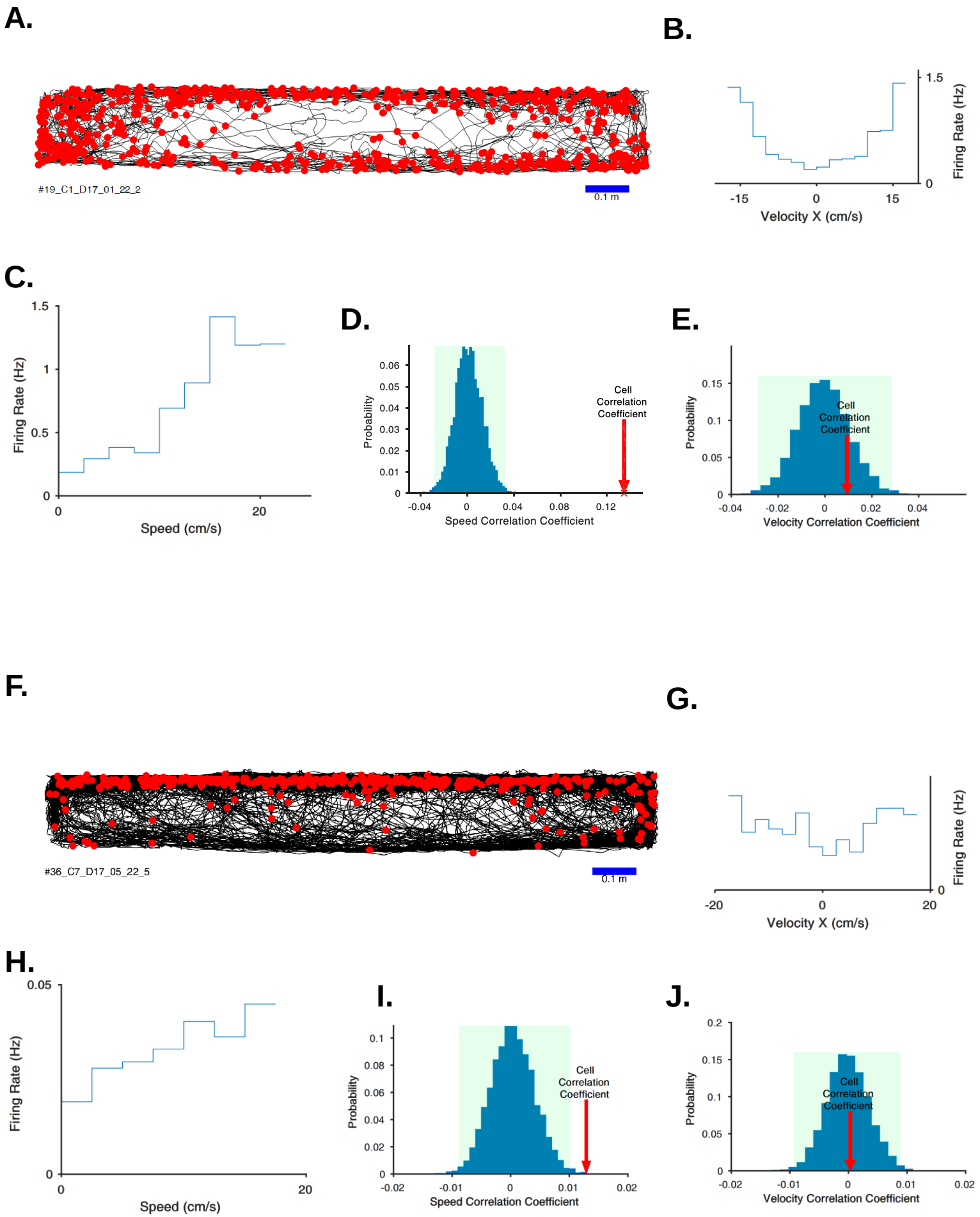

Figure 4 – Vinepinsky et al

Border Velocity Cell

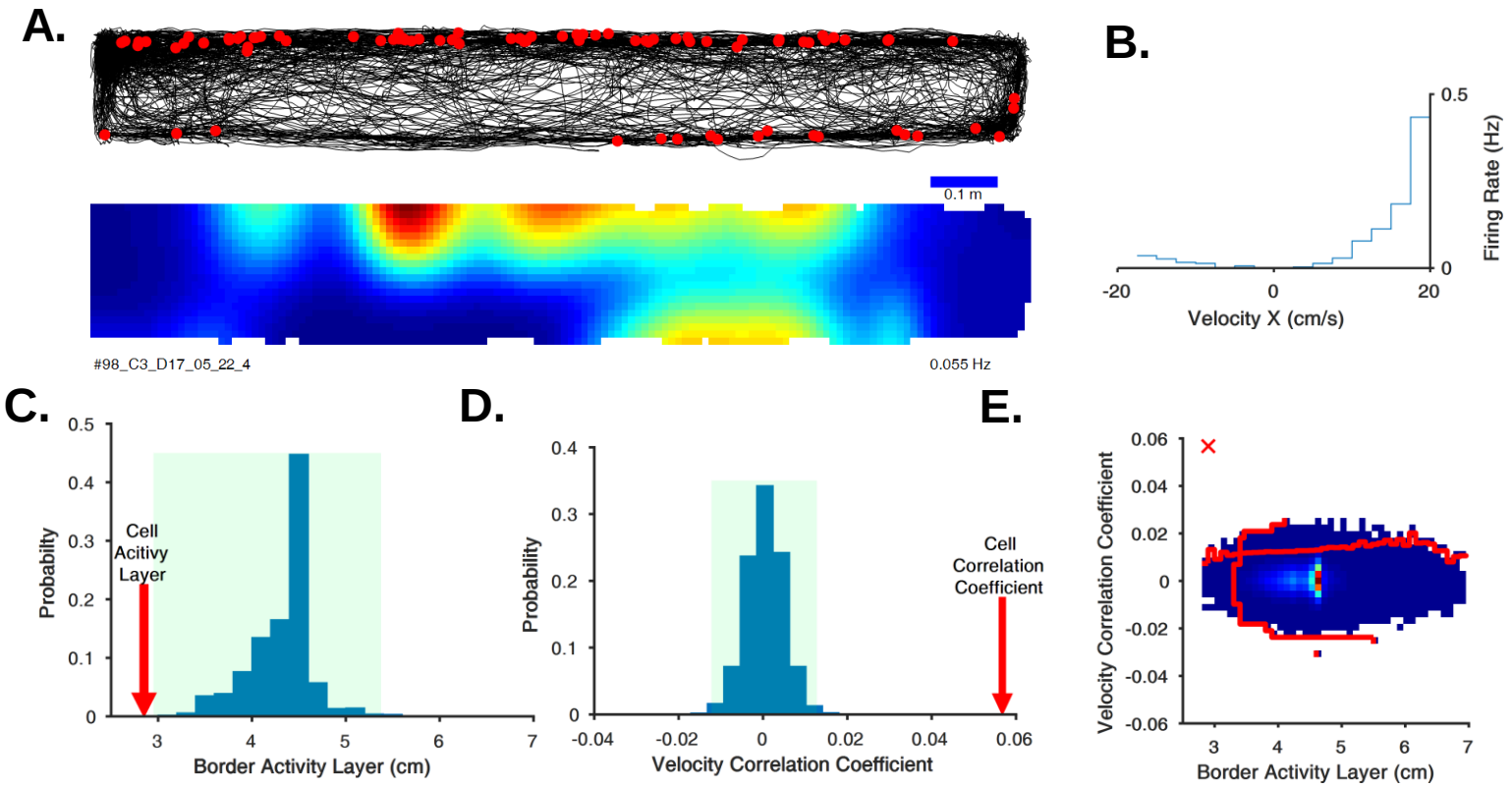

Border Speed Cell

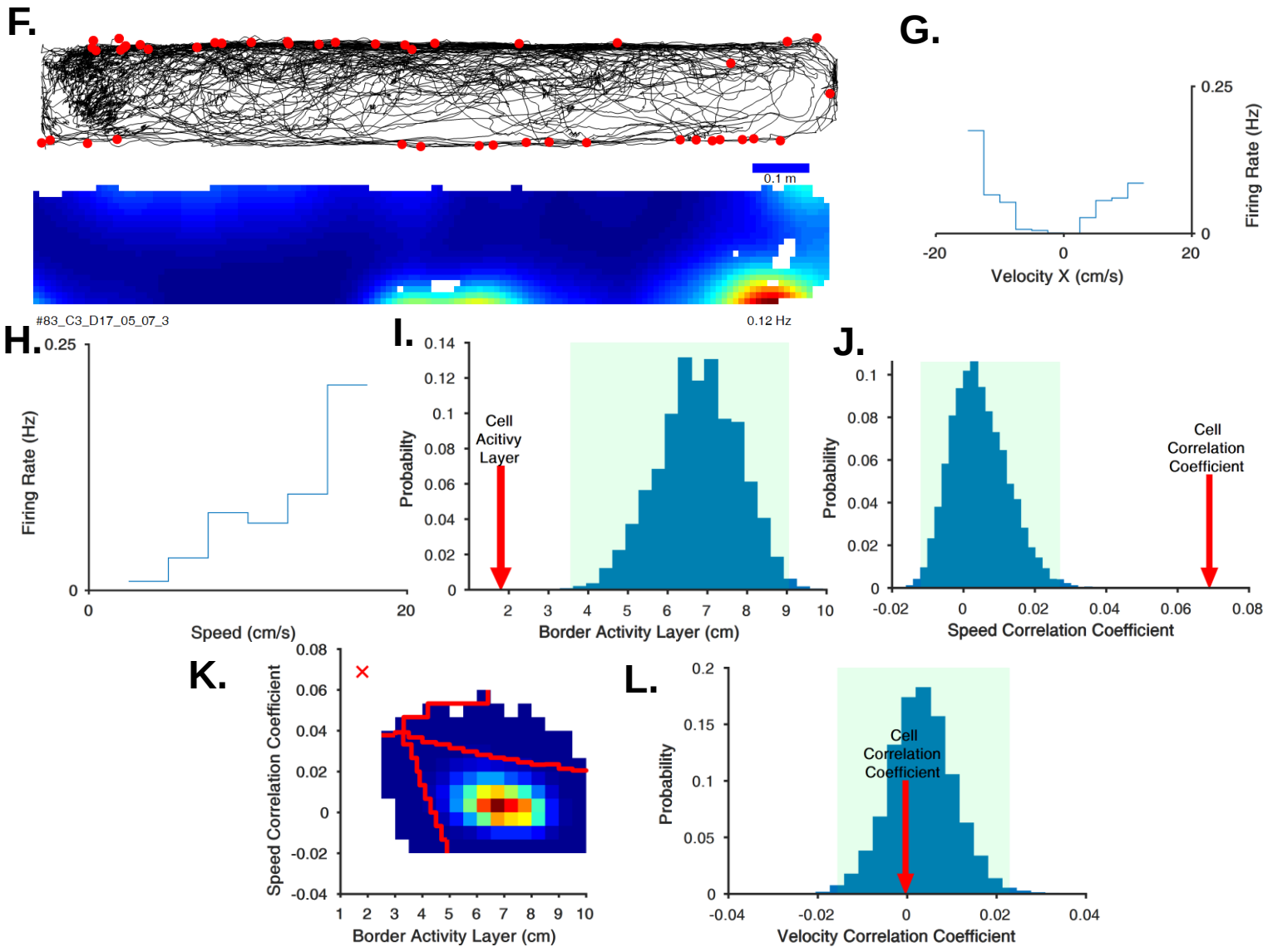

Figure 5 – Vinepinsky et al

A.

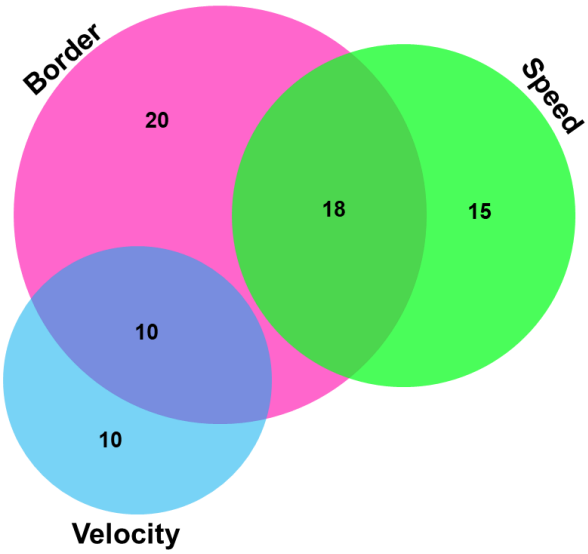

B.

Recording sites

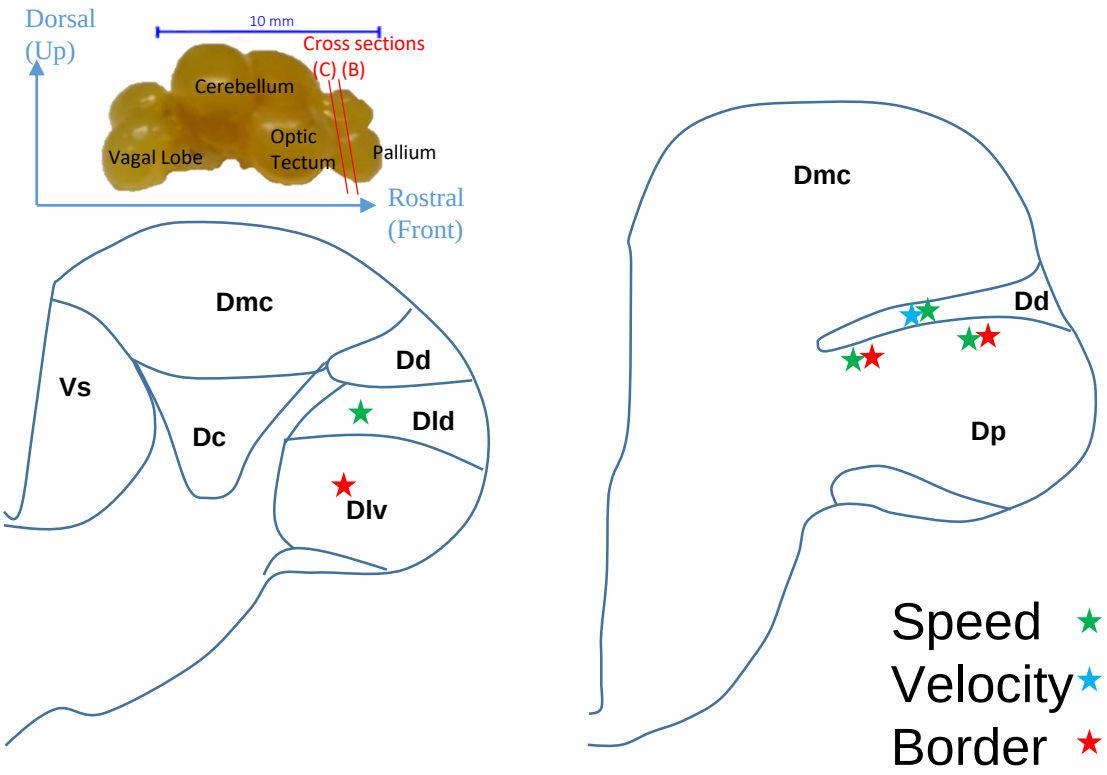

Supplementary Figure 1 – Vinepinsky et al

Border cells examples

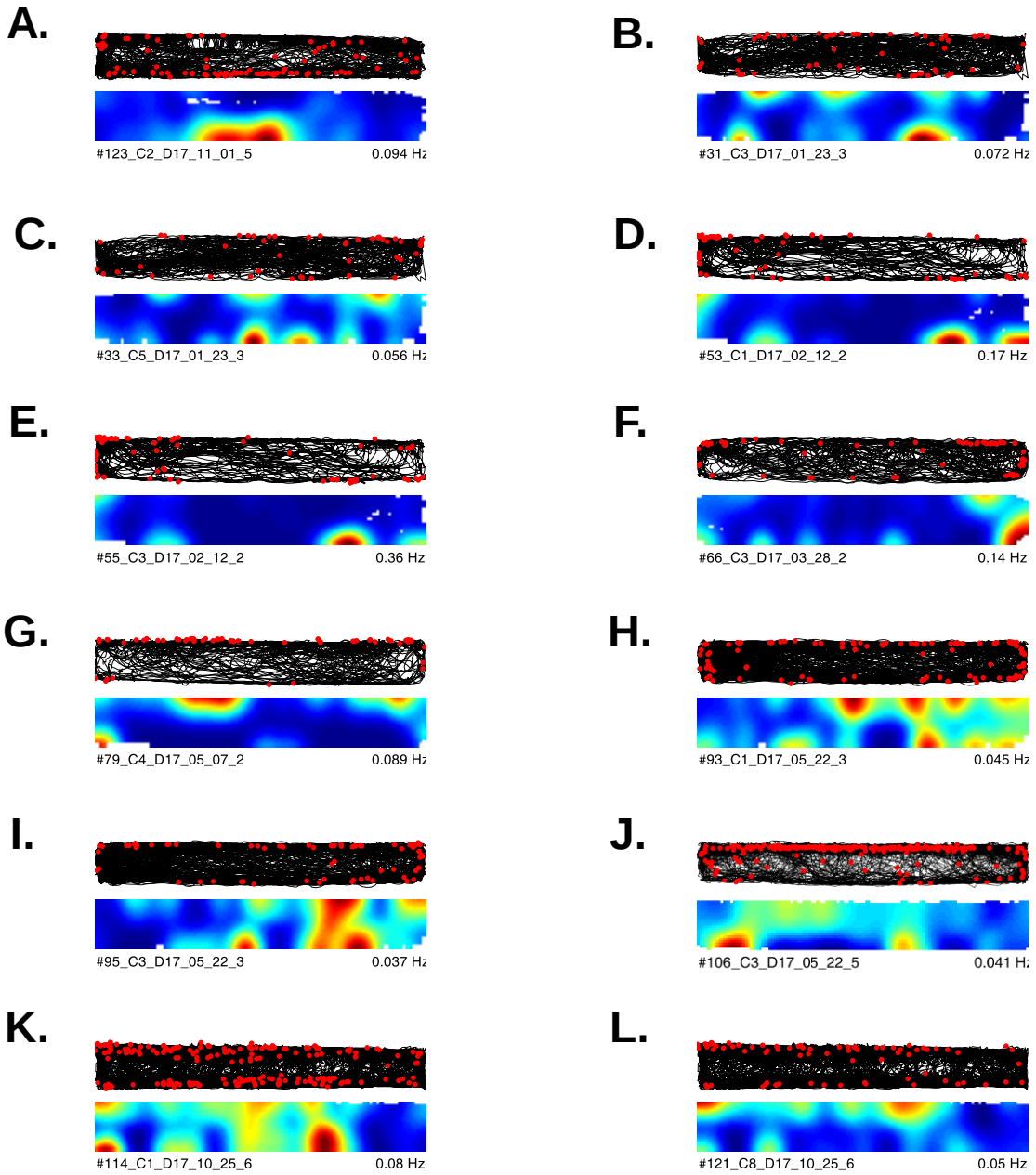

Supplementary Figure 2 – Vinepinsky et al

Firing rate in 2D Velocity Space

Velocity cells

A.

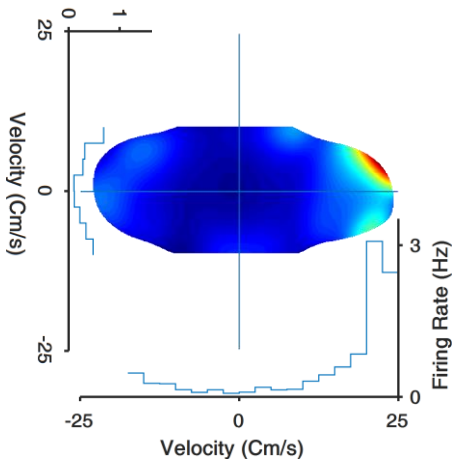

(Corresponded to figure 2C)

B.

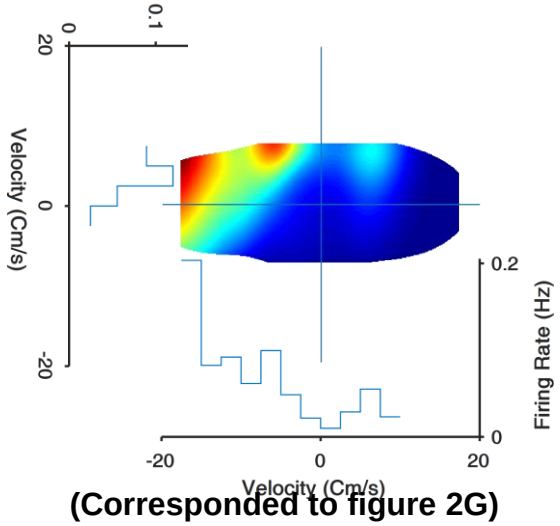

(Corresponded to figure 2G)

Speed cells

C.

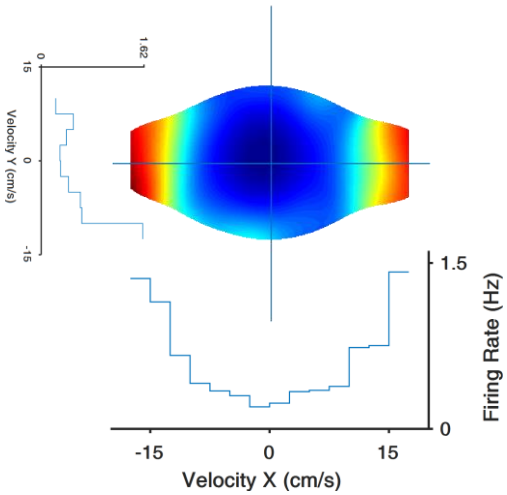

(Corresponded to figure 3B)

D.

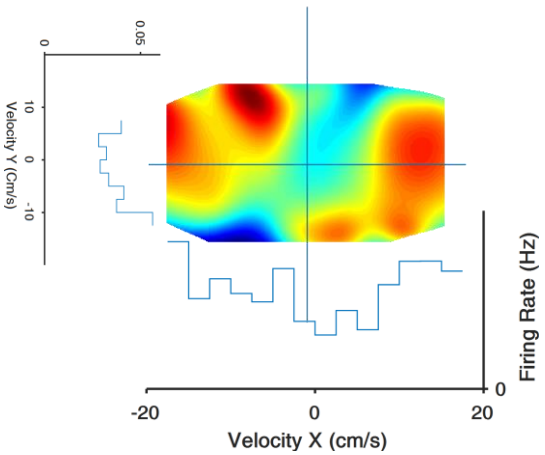

(Corresponded to figure 3G)

Border-Velocity cell

E.

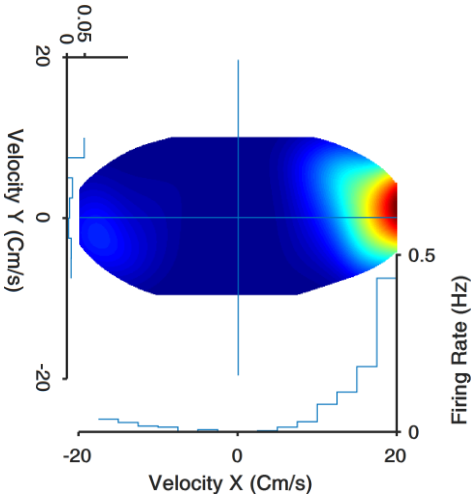

(Corresponded to figure 4B)

Border-Speed cell

F.

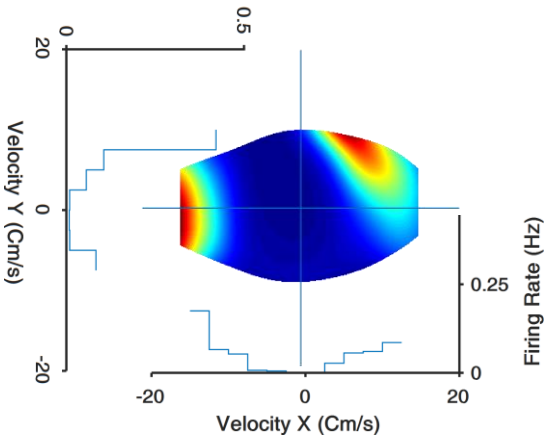

(Corresponded to figure 4G)

Supplementary Figure 3 – Vinepinsky et al

Velocity cells examples

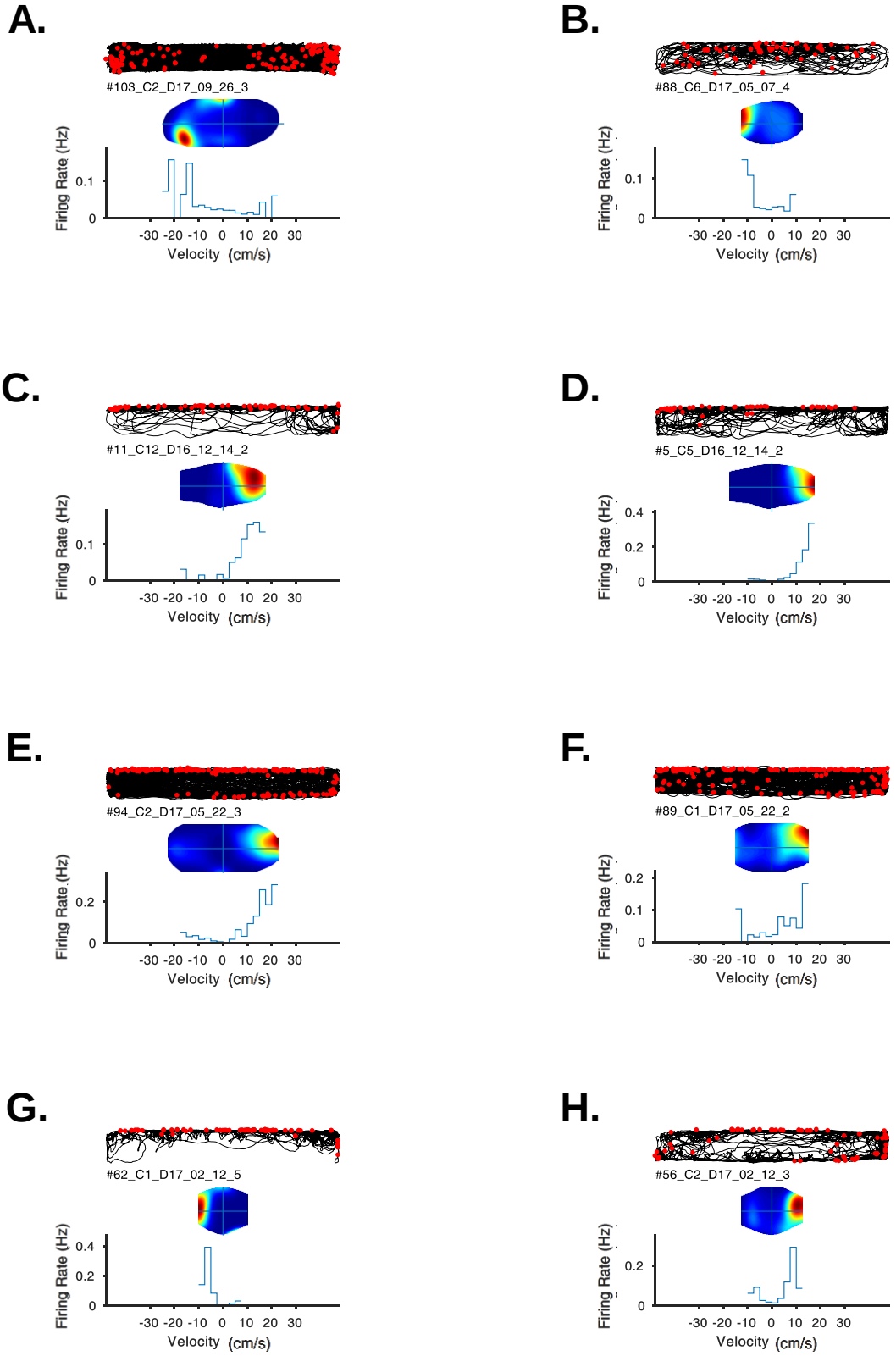

Supplementary Figure 4 – Vinepinsky et al

Speed cells

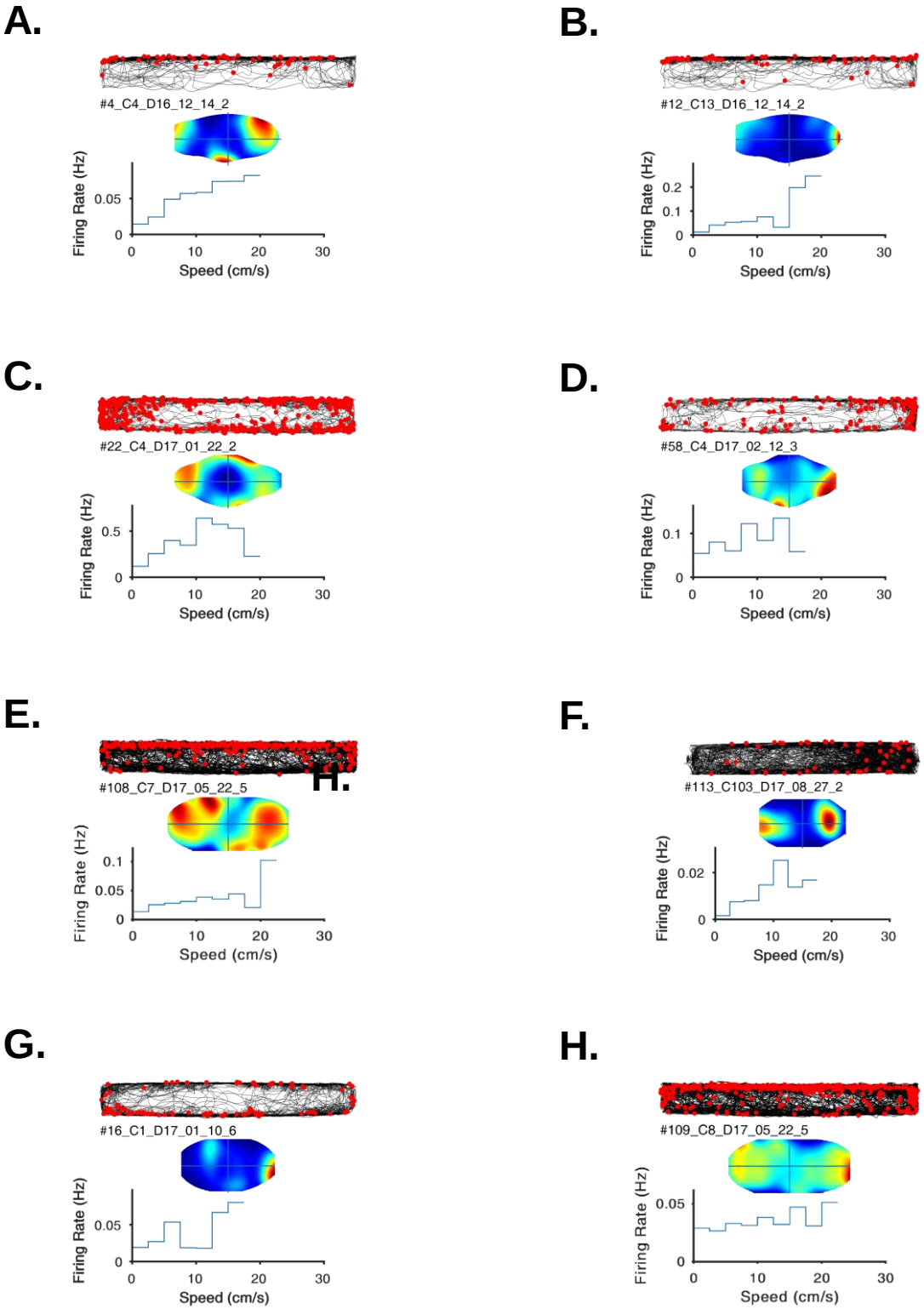

Supplementary Figure 5 – Vinepinsky et al

Border Cell Statistics

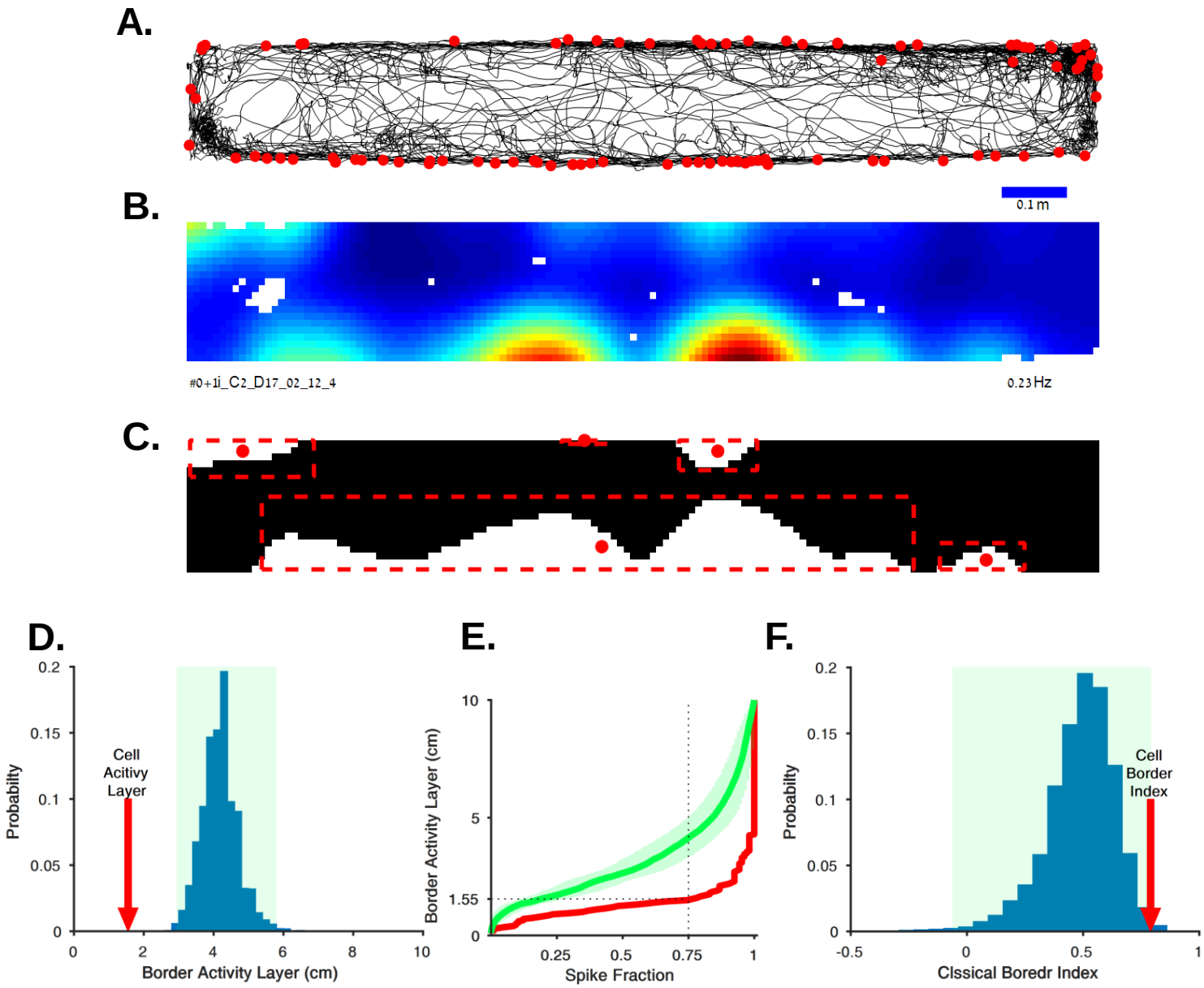

Supplementary Material

Our border cell analysis does not depend on the choice of threshold. In our data, many of the fish exhibited a preference to swim along the borders of the environment (e.g. the cell in Supplementary Figure 5A-B). In addition, many of the neurons had low firing rates. This prompted us to devise a border cell measure based on determining the width of the activity layer near the border that contains 75 % of the spikes (Supplementary Figure 5D). Then by comparing the border distance which contains the 75 % of the spikes (the spike fraction), to the chance value obtained by shuffled data we can place a confidence interval that our observation of border cell is not purely due to chance. To verify that this test does not critically depend on the choice of the 75 % threshold, we analyzed it for all possible thresholds. Supplementary Figure 5E presents two curves of the border distance obtained for the cell (red) and shuffled data (green, 5000 spike trains) as a function of the spike fraction. Clearly, the border distance is significant regardless of the selection of the spike fraction. Thus, the border analysis does not depend on the choice of threshold.

Comparison of our measure for borders and the classical measure. Our measure for border cells coincides with the classical measure *(1)* if the firing rate is high enough (Supplementary Figure 5C-F).

Figure captions for supplementary figures

Supplementary Figure 1| Additional examples of border cells. The cells were recorded in different sessions in different fish. For each cell, the trajectory (black curve) and action potentials (red dots) are presented in addition to a heat map representing the probability of firing in each space bin.

Supplementary Figure 2| The velocity tuning of the cell can be summarized in the color-coded firing rate map as a function of two- dimensional velocity. The dependence of the firing rate on the velocity in two dimensions for the cells in the main text together with the one-dimensional projections. The longitudinal axis is presented in the bottom panels and the crosswise axis in the left panel.

Supplementary Figure 3| Additional examples of velocity cells. The cells were recorded in different sessions in different fish. For each cell, the trajectory (black curve) and action potentials (red dots) are presented in addition to velocity tuning in the longitudinal direction of the neuron.

Supplementary Figure 4| Additional examples of speed cells. The cells were recorded in different sessions in different fish. For each cell, the trajectory (black curve) and action potentials

(red dots) are presented in addition to speed tuning in the longitudinal direction and speed tuning along the same axis.

Supplementary Figure 5| Analysis of border cells. A-C. A sample border cell: trajectory and activity scatter plot (**A**), heat map of spiking probability given position (**B**) and binary activity map (**C**) obtained by putting a 75% threshold on the heat map to obtain the firing fields of the cells (based on*(1)*). **D.** Statistical analysis of the activity near the border of the cell in **A-C.** We compare the border activity layer of the cell that capture 75% of the spikes near the border (red arrow) to the border distance of 5000 shuffled spike trains. The cell has a higher probability of being activated near the boundary than expected by chance ($p<0.005$ in this case). **E.** The neuron activity layer as we varied the spike fraction threshold (red curve) together with the shuffled spike train results (green shading represents the distribution). The selection of the 75 % threshold does not influence the result since we can select a wide range of thresholds and the neuron is still differentiated from the shuffled distribution **F**. The classical analysis of the cell in A-C as in *(1)*. The cell has a significantly high border index.

References

1. T. Solstad, C. N. Boccara, E. Kropff, M. B. Moser, E. I. Moser, Representation of geometric borders in the entorhinal cortex. *Science.* **322**, 1865-1868 (2008).